Arch. Metall. Mater. **70** (2025), 1, 147-153

DOI: https://doi.org/10.24425/amm.2025.152528

SUDEEP KUMAR JAIN[1*], Q. MURTAZA[1], P. SINGH[1]

CMT ASSISTED WIRE ARC ADDITIVE MANUFACTURING OF SS 316L: FABRICATION, CHARACTERIZATION, AND FRACTOGRAPHY

CMT-WAAM, an advanced manufacturing technology, garners significant attention due to its ability to fabricate intricate components efficiently. In this investigation, a 40-layered structure was manufactured from SS 316L using the CMT-WAAM process, with the utilization of optimized process parameters. This research involved the analysis of microstructure and mechanical properties, including microhardness, tensile testing, and fractography, for both WAAM and wrought SS 316L. The UTS of WAAM reached 592.31 MPa and YS of 276.46 MPa, outperforming the UTS of wrought 316L, which was 557.62 MPa, and YS of 284.35 MPa. The PE of WAAM was 59.85%, while for wrought 316L, it was 53.20%, indicating that wrought 316L demonstrated a higher ductility than the WAAM part. The microhardness profile of WAAM showed an average value of 238.14 HV, indicating a 28% increase compared to the MH of wrought 316L, which was measured at 192.37 HV. The microstructure of CMT-WAAM displays δ-ferrite and γ-austenite, along with skeletal and lathy ferrites, similar in wrought 316L. The fractography analysis of tensile specimens exhibited numerous dimples, indicating favorable ductility in the fabricated structure. Therefore, the findings indicate that the CMT-WAAM process meets industrial requirements.

Keywords: WAAM; SS 316L; Tensile Test; Microhardness; Fractography

1. Introduction

WAAM stands out as a state-of-the-art technology for manufacturing large-scale metallic components across diverse industries including automotive, aerospace and shipbuilding. It presents a feasible alternative to conventional manufacturing methods by offering shorter lead times, minimal material wastage, and cost-effectiveness [1-3]. In the wire arc additive manufacturing (WAAM) process, an electric arc is employed to heat and melt the wire, which is then transferred into the molten metal pool. As the molten metal solidifies at the boundary of the melt pool, the part is gradually built layer-by-layer [4]. The WAAM process depends on the type of arc-based welding technology utilized for melting the feed wire and generating a three-dimensional object layer by layer [5]. Presently, wire arc additive manufacturing (WAAM) stands as a promising fabrication process for a range of engineering materials including titanium, aluminum, nickel alloy, and steel [6]. Compared to traditional subtractive manufacturing approaches, WAAM systems offer the potential to cut down fabrication time by 40 to 60% and post-machining time by 15 to 20%, with the degree of reduction influenced by the size of the component [7].

The CMT process, pioneered by Fronius in 2004, signifies an advancement within the realm of gas metal arc welding (GMAW). Its foundation in the short-circuiting transfer process sets it apart from conventional GMAW techniques, particularly in its unique approach to droplet detachment from the feedstock wire [8]. With the incorporation of CMT into wire arc additive manufacturing (WAAM), numerous sectors have experienced substantial benefits attributed to reduced heat transfer and spatter-free operation, leading to enhanced surface quality and the attainment of near-net shapes [9]. 316L stainless steel finds widespread application across diverse sectors including architecture, aerospace, naval, construction, nuclear reactors, oil & gas, cryogenics, and bio-medical fields. This preference is due to its exceptional processability, robust mechanical properties, resistance to corrosion, and impressive toughness.[10] The microstructural composition of 316L stainless steel encompasses both γ-austenite and δ-ferrite phases, regardless of the fabrication method employed, including casting, welding, and additive manufacturing (AM) [11].

This research paper employs CMT-WAAM to fabricate a multilayer structure using 316L stainless steel. The study includes examinations of microstructural analysis and mechanical

[1] DELHI TECHNOLOGICAL UNIVERSITY, DEPARTMENT OF MECHANICAL ENGINEERING, DELHI-110042 (INDIA)

* Corresponding Author: sudeepjain16@gmail.com

TABLE 1

Chemical composition SS 316L wire (weight %)

Elements	Cr	Ni	Mo	C	Mn	S	Si	P	Cu	Fe
Wt. (%)	18.56	11.55	2.53	0.01	1.53	0.01	0.59	0.027	0.17	Rest

properties, with a focus on comparing the outcomes to those of wrought 316L material.

2. Materials and method

For the WAAM process, an SS-316L base plate measuring 200×50×6 mm and an SS-316L filler wire with a diameter of 1.2 mm were selected. The chemical composition (% weight) of the base material and the filler wire is provided in TABLE 1. Metal additive manufacturing employed a CMT welding machine (TPS400i) and a KuKa robot (KR 8 R1440) for the process. The setup is described in Fig. 1 and Fig. 2 outlines the WAAM process.

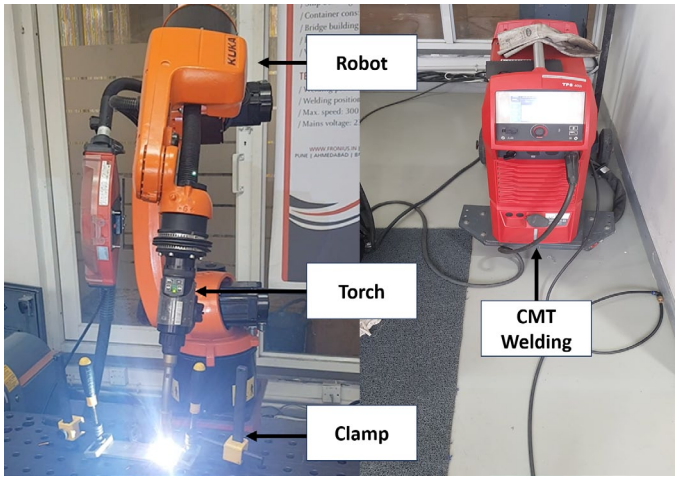

Fig. 1. CMT WAAM setup

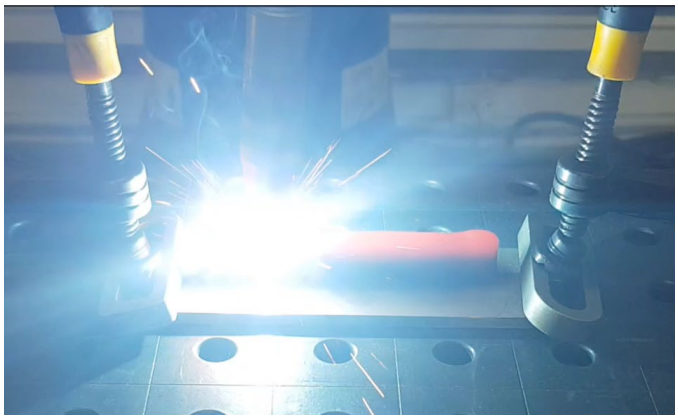

Fig. 2. WAAM sample under fabrication

The experimental setup maintained a gas mixture of 97% Ar and 3% CO_2 99.99% of purity level. The flow rate was regulated at 15 liters per minute, and the CTWD was maintained at 3.0 mm. To establish welding parameters, preliminary weld trials were performed. Lower currents resulted in inadequate weld penetration and fusion, whereas currents above 130 A caused an increase in sample thickness. The experiment was conducted at 0.7 mm speed. After extensive trial runs and a comprehensive literature review, the optimal current settings were identified and tabulated in TABLE 2. For microstructural analysis, 10×10 coupons were extracted from both WAAM and wrought steel. The microstructural characterization was conducted by adhering to a standard metallography procedure. The samples were etched by immersing them in a solution containing 30 ml of HCl, 120 ml of distilled water, and 10 g of $FeCl_3$ [12]. The microstructural analysis involved the utilization of an Olympus GX 41 optical microscope and a Zeiss (Gemini 2) FESEM. The Vickers Microhardness assessments were carried out using a Struers instrument (Model: Duramin-40 M1) at a load of 500 g and a dwell time of 10 s, following the ASTM E384 standard. Tensile tests were performed on the tensile specimen utilizing a universal testing machine, INSTRON instrument (Model: 3380, USA). Tensile test coupons were prepared following the ASTM E8M standard. The UTS, YS, and PE of both WAAM and wrought 316L were measured at 1mm/min crosshead speed.

TABLE 2

Parameters for WAAM fabrication

Parameters	Value
Current (A)	100
welding speed (m/min)	0.7
Voltage (V)	11.4
Wire feed rate (m/min)	3.7
No of layers	40
Contact tip distance (mm)	3.0

3. Result and discussion

3.1. Microstructure

The prominent characteristic observed in the CMT-WAAM 316L samples was their multilayered microstructure, primarily resulting from the intricate thermal histories involved. The multilayered structure exhibited alterations in ferrite, austenite, and residual stress. Fig. 3(a) shows optical micrographs illustrating the occurrence of the WAAM sample's δ-ferrite phase, depicted in black and distributed within the γ-austenite matrix, with grain growth predominantly occurring in the vertical direction. During the preliminary stages of solidification, ferrite served as the primary phase precipitating from the liquid phase, followed by a distinct enrichment of Cr and Mo atoms on the δ-ferrite.

As ferrite grows, there is a simultaneous and ongoing release of Ni atoms from the ferrite into the liquid phase, thereby establishing a favorable environment for the subsequent formation of γ-austenite [13]. Continuous deposition-induced heat accumulation, compounded by the concurrent cooling effect of the shielding gas, produced a subrapid cooling rate for the liquid alloy due to the cumulative thermal effects. Such thermal conditions led to a solidification behavior in the alloy characterized by the concurrent existence of the γ-austenite and δ-ferrite phases. In the early solidification stages, liquid metal witnessed the formation of high-temperature δ-ferrite. Following this, a transformation occurred where a segment of the δ-ferrite, along with the surrounding liquid, underwent a peritectic conversion into γ-austenite. Residual liquid at that point solidified directly, resulting in the formation of γ-austenite. Ongoing heat accumulation prompted the transformation of some primary δ-ferrite phases into γ-austenite. The residual ferrites were then dispersed within the austenitic matrix, forming a net-like and skeletal structure [14]. The FESEM image shown in Fig. 3(b), the WAAM's microstructure, demonstrates a ferrite-austenite mode. In this microstructure, γ-austenite serves as the primary phase, while δ-ferrite at the grain boundaries of γ-austenite. Both lathy (parallel structure) and skeletal (dispersed structure) structures were observed in δ-ferrite. Within the microstructure, a substantial enrichment of Cr (24.8%) and Ni (4.06%) is unveiled through the EDX analysis results plot and chemical spectrum presented in Fig. 4.

3.2. Microhardness

Microhardness tests were conducted at seven positions spanning from the bottom (near the base) to the top, as depicted in Fig. 5. It was observed that the hardness steadily reduced from the base to the top due to a non-uniform temperature distribu-

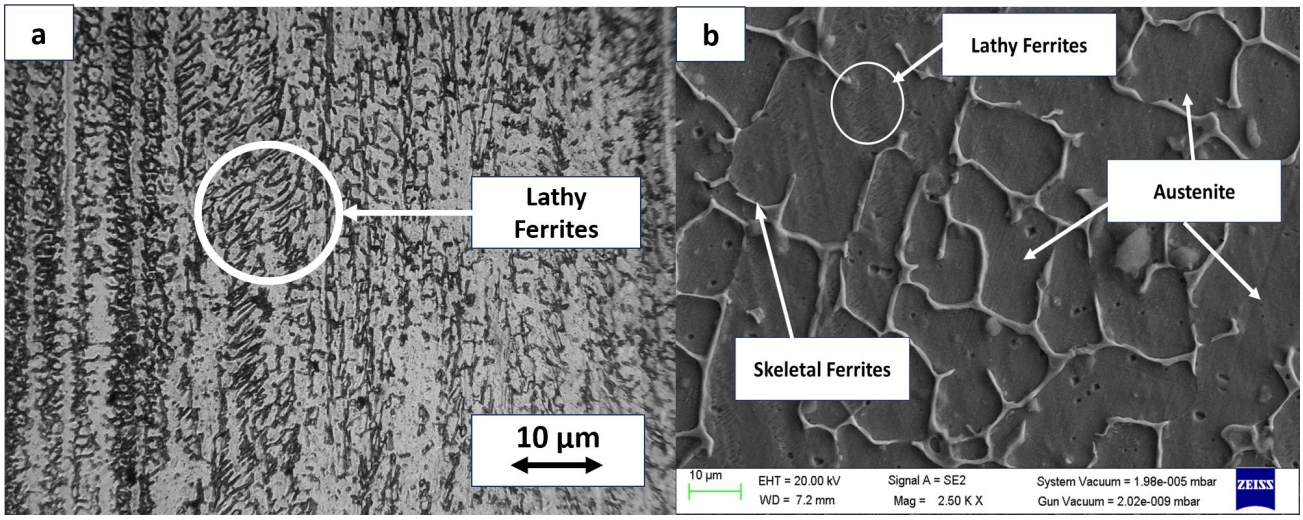

Fig. 3. (a) Optical Microscopy of WAAM sample, (b) FESEM of WAAM sample

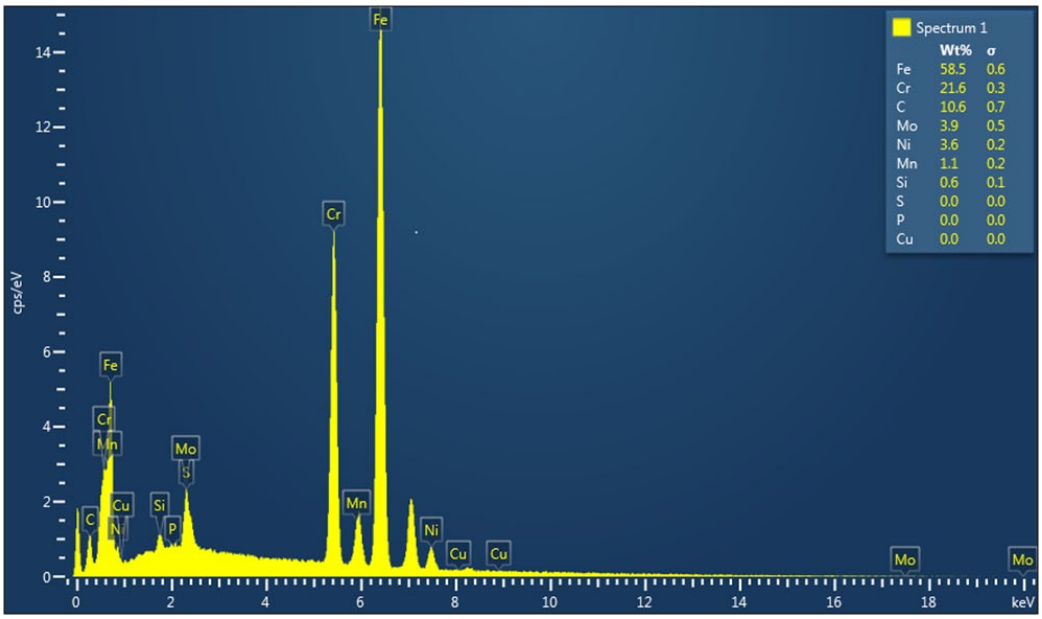

Fig. 4. EDX plot of WAAM sample

tion [15]. Microhardness evaluation conducted on the WAAM sample reveals an average value of 242.74 HV near the base, followed by a midrange value of 231.57 HV in the middle zone. The top zone exhibits an average microhardness measurement of 217.24 HV. The WAAM sample displayed a maximum hardness value of 246.63 HV near the base, with the lowest value of 209.10 HV measured at the top. Compared to the top and middle zones, there was a slight increase in microhardness observed in the bottom zone, which is likely associated with the larger heat dissipation from the substrate plate. The uniformity in hardness values across all zones suggests consistent behavior within the built structure, reducing the potential for brittle failure. In contrast, as time passes, there is a substantial increase in heat accumulation between layers, leading to a gradual decline in hardness [16]. It has been found that the average microhardness of the SS 316L WAAM is larger than the wrought 316L, which has a hardness of 192 HV. This observation is supported by numerous studies in the literature, indicating that the microhardness of additive-manufactured parts of 316L SS is generally higher than the conventionally manufactured 316L SS parts [17].

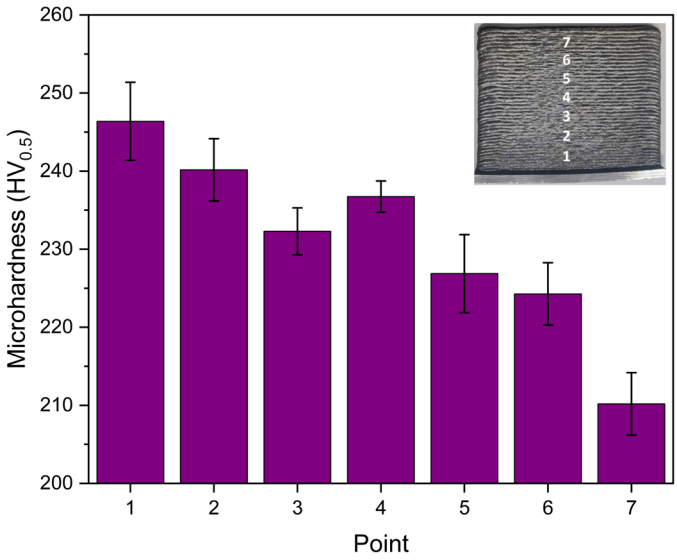

Fig. 5. Microhardness plot of WAAM sample

3.3. Tensile testing

Tensile testing was performed on both SS 316L WAAM and wrought SS 316L, with the results visually depicted in Fig. 6. SS 316L WAAM ultimate tensile strength (UTS) measured 592.31 MPa, accompanied by a yield strength (YS) of 276.46 MPa. Additionally, the wrought steel ultimate tensile strength was measured at 557.62 MPa with a yield strength of 284.39 MPa. SS 316L WAAM showcased superior tensile strength of a 6.28% increment in performance when compared to the wrought material. In comparison, the WAAM part exhibited a percentage elongation of 53.20%, while conventional manufactured steel recorded a slightly higher percentage elongation of 59.85%. The changes observed in the tensile properties of the SS316L WAAM can be primarily attributed to the heterogeneous microstructural modifications arising from the thermal stresses encountered during the manufacturing of multilayer structures [18]. Kumar et al. in their research for SS 316L reported similar results [19]. Fig. 7 demonstrates the bar chart for the comparison of tensile properties of WAAM and wrought 316L.

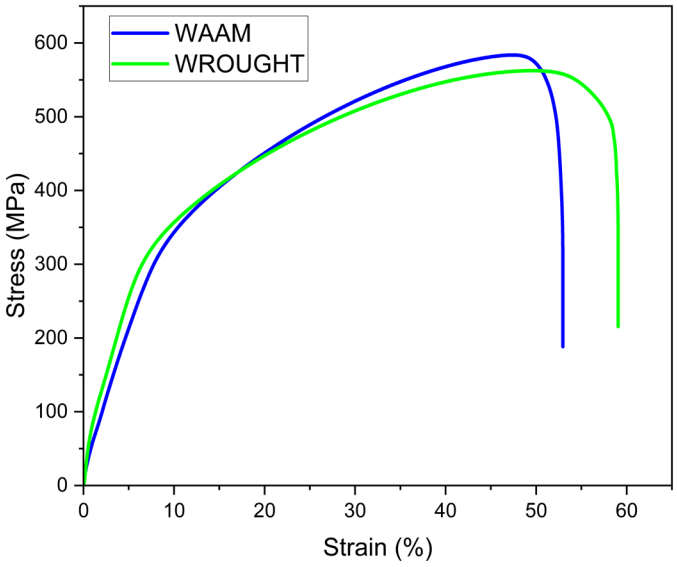

Fig. 6. Stress-Strain curve for WAAM and Wrought SS 316L

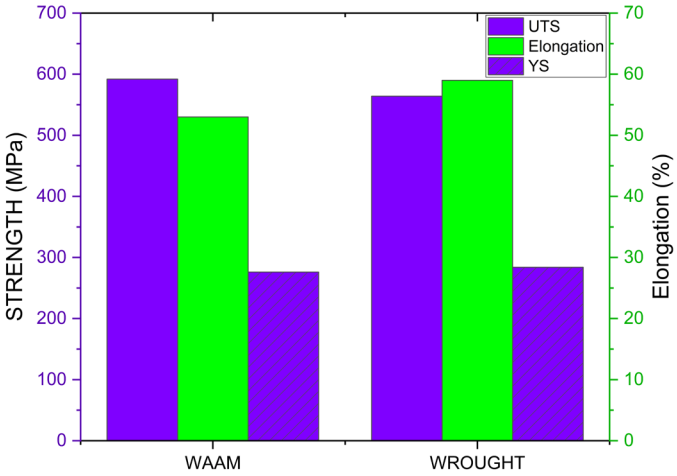

Fig. 7. Bar chart of Tensile properties of WAAM and Wrought 316L

3.4. Fractography

The fracture surfaces are illustrated in Fig. 8(a) and the FESEM fractography of tensile coupons for WAAM and wrought 316L are illustrated in Figs. 8(b) and 8(c). The fractured surface of the tensile specimens revealed distinct signs of equiaxed dimples and void deposition across the layers. A significant number of dimples, evenly distributed across the fracture surface, confirmed a ductile fracture mode and implied satisfactory toughness in the as-formed materials [20]. The EDS graph for WAAM and wrought steel is presented in Figs. 9(a) and 9(b). EDS results concluded that the oxygen weight percentage for the WAAM and wrought steel was 1.4 and 1.3% respectively,

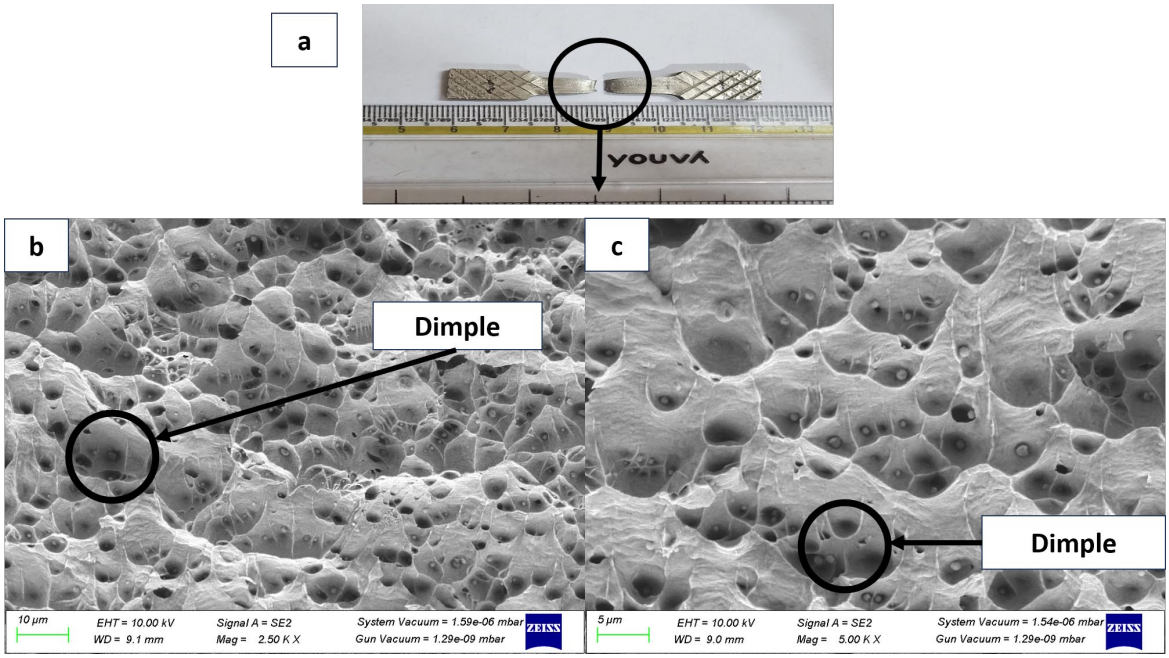

Fig. 8. (a) Fracture image of Tensile Specimen, (b) FESEM of WAAM, (c) FESEM of Wrought 316L

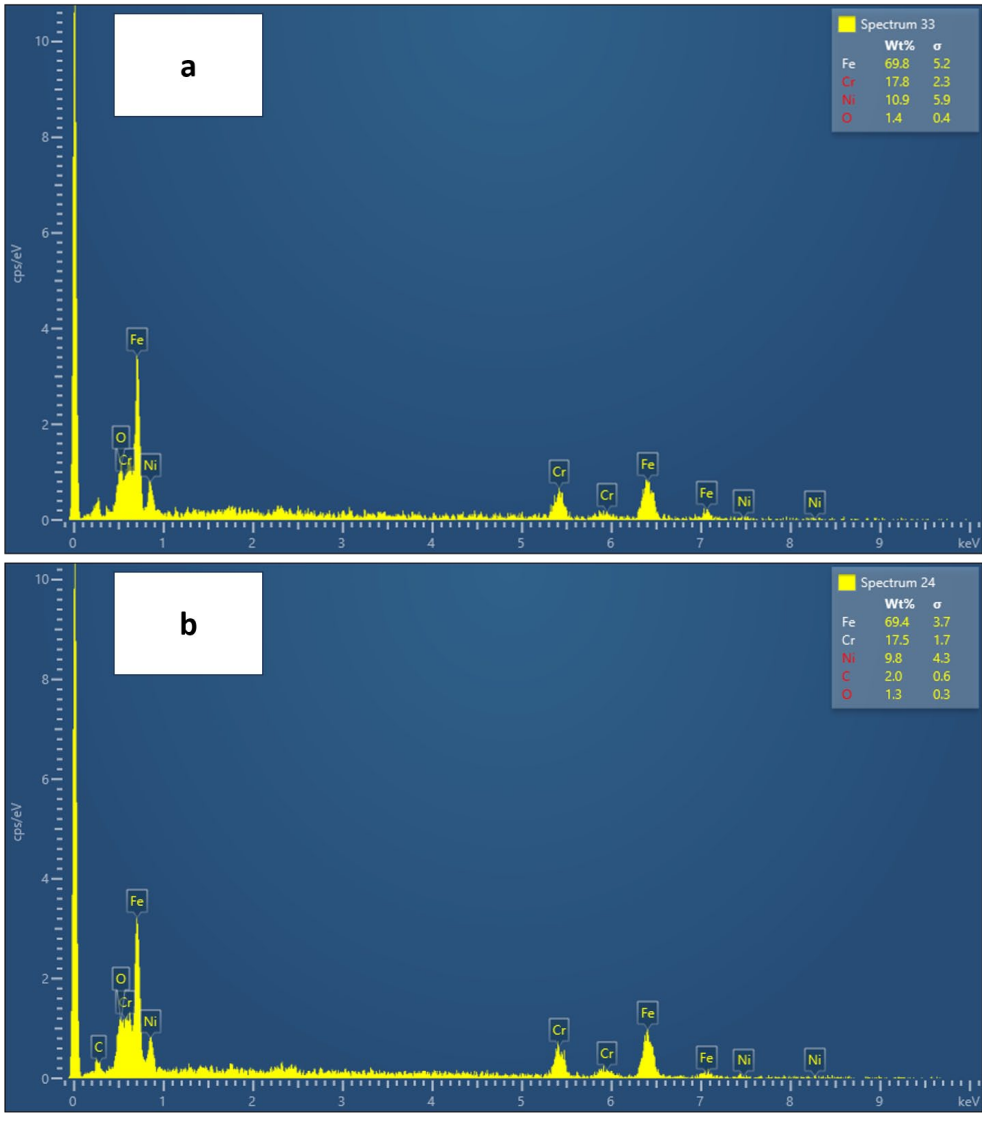

Fig. 9. (a) EDS WAAM, (b) EDS Wrought 316L

indicating a low level of oxidation. A significant presence of oxygen implies that the oxidizing impurities are present within the dimples, which generally act as a source of brittleness and serve as initiation of cracks [21].

4. Conclusions

WAAM, particularly utilizing CMT technology, is gaining traction due to its affordability, fast deposition rates, and capacity for large-scale component fabrication. This method boasts advantages including lesser heat, minimal distortion due to thermal residual stresses and reduced operational costs, this approach emerges as a promising choice for industrial usage. In this work, the CMT-WAAM process was employed to manufacture a 40-layered structure from SS 316L using optimized process parameters and SS316L metal wire. The examination of microstructure and mechanical properties such as tensile testing, microhardness, and fractography was conducted for both WAAM and wrought 316L in this research. The key findings of the current research are outlined below.

1. The fabricated multi-layered structure showed seamless fusion and no disbonding. Analysis of the macrostructure provided evidence of seamless fusion without oxidation or defects, ensuring structural integrity.
2. The microstructure of the CMT-WAAM reveals the presence of both δ ferrite and γ austenite, with skeletal and lathy ferrites observed. Similar results were observed in wrought 316L.
3. The tensile properties analysis revealed that the WAAM process produced results within the range of values observed for wrought SS 316L. WAAM SS316L exhibited higher average UTS and YS values at 592.31 MPa and 276.46 MPa, respectively, compared to 557.62 MPa and 284.39 MPa for wrought 316L. However, the elongation of wrought 316L, at 59.85%, exceeded that of WAAM SS316L, which was recorded at 53.2%.
4. Across the top zone, middle zone, and bottom zones, SS 316L WAAM sample exhibited microhardness values of 242.74 HV, 231.57 HV, and 217.24 HV, respectively, outperforming wrought 316L at 192 HV. Despite these differences, uniform microhardness behavior was observed throughout the built structure, indicating resilience against brittle failure.
5. FESEM examination of fractured tensile specimens revealed closely packed large dimples, underscoring the superior ductility of the multilayered structure. Additionally, EDX analysis revealed a reduced oxygen content, lowering the potential for brittle fracture.

Nomenclature

WAAM – Wire Arc Additive Manufacturing
CMT – Cold Metal Transfer
WS – Welding speed
CTWD – Contact Tip to Work Distance
UTS – Ultimate Tensile Strength
YS – Yield Strength
PE – Percentage Elongation
MH – Microhardness

REFERENCES

[1] L.P. Raut, R.V. Taiwade, Wire Arc Additive Manufacturing: A Comprehensive Review and Research Directions. J. Mater. Eng. Perform. **30**, 7, 4768-4791, Jul. (2021). DOI: https://doi.org/10.1007/s11665-021-05871-5

[2] H. Pant, A. Arora, G.S. Gopakumar, U. Chadha, A. Saeidi, A. E. Patterson, Applications of wire arc additive manufacturing (WAAM) for aerospace component manufacturing. The International Journal of Advanced Manufacturing Technology **127**, 11-12, 4995-5011, Aug. (2023). DOI: https://doi.org/10.1007/s00170-023-11623-7

[3] B.O. Omiyale, T.O. Olugbade, T.E. Abioye, P.K. Farayibi, Wire arc additive manufacturing of aluminium alloys for aerospace and automotive applications: A review. Materials Science and Technology **38**, 7, 391-408, May (2022). DOI: https://doi.org/10.1080/02670836.2022.2045549

[4] A. Shah, R. Aliyev, H. Zeidler, S. Krinke, A Review of the Recent Developments and Challenges in Wire Arc Additive Manufacturing (WAAM) Process. Journal of Manufacturing and Materials Processing **7**, 3, 97, May (2023). DOI: https://doi.org/10.3390/jmmp7030097

[5] IvánTabernero, A. Paskual, P. Álvarez, A. Suárez, Study on Arc Welding Processes for High Deposition Rate Additive Manufacturing. Procedia CIRP **68**, 358-362 (2018). DOI: https://doi.org/10.1016/j.procir.2017.12.095

[6] B. Tomar, S. Shiva, T. Nath, A review on wire arc additive manufacturing: Processing parameters, defects, quality improvement and recent advances. Mater. Today Commun. **31**, p. 103739, Jun. (2022). DOI: https://doi.org/10.1016/j.mtcomm.2022.103739

[7] B. Wu et al., A review of the wire arc additive manufacturing of metals: properties, defects and quality improvement. J. Manuf. Process **35**, 127-139, Oct. (2018). DOI: https://doi.org/10.1016/j.jmapro.2018.08.001

[8] Xizhang Chen et al., Cold Metal Transfer (CMT) Based Wire and Arc Additive Manufacture (WAAM) System. Journal of Surface Investigation: X-ray, Synchrotron and Neutron Techniques **12**, 6, 1278-1284, Nov. (2018). DOI: https://doi.org/10.1134/S102745101901004X

[9] B. Tomar, S. Shiva, Cold metal transfer-based wire arc additive manufacturing. Journal of the Brazilian Society of Mechanical Sciences and Engineering **45**, 3, 157, Mar. (2023). DOI: https://doi.org/10.1007/s40430-023-04084-2

[10] P.S. Gowthaman, S. Jeyakumar, D. Sarathchandra, Effect of Heat Input on Microstructure and Mechanical Properties of 316L Stainless Steel Fabricated by Wire Arc Additive Manufacturing. J. Mater. Eng. Perform. **33**, 5536-5546, May (2023). DOI: https://doi.org/10.1007/s11665-023-08312-7

[11] X. Chen, J. Li, X. Cheng, B. He, H. Wang, Z. Huang, Microstructure and mechanical properties of the austenitic stainless steel 316L fabricated by gas metal arc additive manufacturing. Materials Science and Engineering: A, **703**, 567-577, Aug. (2017). DOI: https://doi.org/10.1016/j.msea.2017.05.024

[12] V. Mishra, N. Yuvaraj, Vipin, Tribological Behaviour of Austenitic Stainless Steel-Clad Surface Over Low Carbon Steel Produced by Cold Metal Transfer Welding Process. Transactions of the Indian Institute of Metals, Feb. (2024). DOI: https://doi.org/10.1007/s12666-024-03261-8

[13] J. Lei, J. Xie, S. Zhou, H. Song, X. Song, X. Zhou, Comparative study on microstructure and corrosion performance of 316 stainless steel prepared by laser melting deposition with ring-shaped beam and Gaussian beam. Opt. Laser Technol. **111**, 271-283, Apr. (2019). DOI: https://doi.org/10.1016/j.optlastec.2018.09.057

[14] B. Xie, J. Xue, X. Ren, Wire Arc Deposition Additive Manufacturing and Experimental Study of 316L Stainless Steel by CMT + P Process. Metals (Basel) **10**, 11, 1419, Oct. (2020). DOI: https://doi.org/10.3390/met10111419

[15] N. Brubaker et al., Investigating Microstructure and Properties of 316L Stainless Steel Produced by Wire-Fed Laser Metal Deposition. J. Mater. Eng. Perform. **31**, 5, 3508-3519, May (2022). DOI: https://doi.org/10.1007/s11665-021-06477-7

[16] S. Mahendiran, R. Ramanujam, Investigation of Surface Residual Stress, Mechanical Properties, and Metallurgical Characterization of Inconel 625 Multilayer Thin-Wall Component Using Cold Metal Transfer Technique. J. Mater. Eng. Perform., Jan. (2024). DOI: https://doi.org/10.1007/s11665-023-09119-2

[17] S. Yusuf, Y. Chen, R. Boardman, S. Yang, N. Gao, Investigation on Porosity and Microhardness of 316L Stainless Steel Fabricated by Selective Laser Melting. Metals (Basel) **7**, 2, 64, Feb. (2017). DOI: https://doi.org/10.3390/met7020064

[18] L.B.O. Souza, M.R.N. Santos, R.P. Garcia, D.B. Fernandes, L.O. Vilarinho, Characterization of an austenitic stainless steel preform deposited by wire arc additive manufacturing. The International Journal of Advanced Manufacturing Technology **123**, 9-10, 3673-3686, Dec. (2022). DOI: https://doi.org/10.1007/s00170-022-10382-1

[19] V. Kumar, S. Dwivedi, A. Mandal, A.R. Dixit, Experimental investigations on the microstructural evolution and their influence on mechanical, tribological and corrosion performance of wire-arc additive manufactured SS316L structure. Mater. Today Commun. **38**, 107673, Mar. (2024). DOI: https://doi.org/10.1016/j.mtcomm.2023.107673

[20] C. Sasikumar, R. Oyyaravelu, Mechanical properties and microstructure of SS 316 L created by WAAM based on GMAW. Mater. Today Commun. **38**, 107807, Mar. (2024). DOI: https://doi.org/10.1016/j.mtcomm.2023.107807

[21] J. Vora, H. Parmar, R. Chaudhari, S. Khanna, M. Doshi, V. Patel, Experimental investigations on mechanical properties of multi-layered structure fabricated by GMAW-based WAAM of SS316L. Journal of Materials Research and Technology **20**, 2748-2757, Sep. (2022). DOI: https://doi.org/10.1016/j.jmrt.2022.08.074